Accepted Manuscript

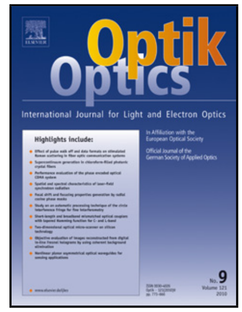

Title: Error separation methods based on absolute testing of non-uniform sampling

Authors: Lu Zhang, Yang Xiang

PII: S0030-4026(18)31136-7
DOI: https://doi.org/10.1016/j.ijleo.2018.08.017
Reference: IJLEO 61314

To appear in:

Received date: 29-10-2016
Revised date: 31-7-2018
Accepted date: 10-8-2018

Error separation methods based on absolute testing of non-uniform sampling

LU ZHANG, [1, 2] YANG XIANG[1,*]

[1] *Changchun Institute of Optics, Fine Mechanics and Physics, Chinese Academy of Sciences, Changchun 130033, China*
[2] *University of Chinese Academy of Sciences, Beijing, 100049, China*

[*]***Corresponding author****: y.xiang@sklao.ac.cn*

Received XX Month XXXX; revised XX Month, XXXX; accepted XX Month XXXX; posted XX Month XXXX (Doc. ID XXXXX); published XX Month XXXX

Abstract
Grating lateral shearing interferometry is one of important technique to test the system wavefront aberration from lithographic lens. In order to achieve the calibration in ultra-high-precision, we must eliminate the system errors from the grating lateral shearing interferometer. Therefore, a three-step average algorithm and a weighed-three-step average algorithm are proposed to remove the rotationally asymmetric system errors from our shearing setup. The research results show that the RMS of the accuracy of three-step average algorithm centered on 45° can approach 0.71nm, and the RMS of the accuracy of its weighed algorithm can approach 0.54nm.

Keywords: absolute calibration; grating lateral shearing interferometer; system errors; rotation algorithm

OCIS codes: *(120.3940) Metrology; (120.4800) Optical standards and testing; (230.1950) Diffraction gratings.*

1. INTRODUCTION

Lithographic lens is the core component of lithography machine, the wavefront aberration from the lens under test will directly influence the lithography function parameters from lithography machine, such as the characteristic line width and the overlay accuracy. Currently, the major methods for testing the wavefront aberration from lithographic lens are: Shark-Hartmann Interferometry [1], Grating Shearing Interferometry [2], Point Diffraction Interferometry [3], and Twyman—Green Interferometry [4], EUV Experimental Interferometry [5], etc. For the lithographic lens in 193nm work wavelength, we usually utilize grating lateral shearing interferometry to measure the wavefront aberration from lithographic lens, owing to the rigorous working condition and the costly expenses.

For achieving the measurement precision in sub-nanometer, it is necessary to ensure and eliminate the system errors from grating lateral shearing interferometer. According to the principle of absolute calibration and the projects for measuring the wavefront aberration of lithographic lens, the shift method [6] and the cat's eye method [7] doesn't work, and we can use the rotation algorithm [8-12] to ensure the rotationally asymmetric system error from the interferometer. Aimed at Twyman—Green interferometry, Mack proposed an error separation technique [4] which is a three-step combination algorithm with φ=0° as base point. Apply this method to the grating lateral shearing interferometer, and we found measurement precision was largely influenced by non-uniform rotation.

In this paper, a three-step average algorithm and a weighted-three-step average algorithm with φ=45° as base point are proposed to decrease the influence of non-uniform sampling to measurement result on grating lateral shearing interferometer.

2. BASIC THEORY

The error separation technique[4] is a three-step combination algorithm which need respectively measure the wavefront aberrations of the lens at original position (φ=0°) and another three rotation angle positions (φ=45°, 90°, and 180°) about the optical axis. The wavefront aberration of the lens contains the system error can be expressed as:

$$W(\rho,\theta|\varphi)=W_S(\rho,\theta)+T(\rho,\theta+\varphi) \qquad (1)$$

where W_s (ρ, θ) represents the constant system error from the interferometer; T (ρ, θ) represents the wavefront aberration of the lens; ρ represents a normalized radial coordinate and θ the azimuthal coordinate. Then the mathematical relationships can be expressed as follows:

$$W(\rho,\theta|0°)+W(\rho,\theta|45°)=T(\rho,\theta)+T(\rho,\theta+45°)+2\cdot W_s(\rho,\theta) \quad (2)$$

$$W(\rho,\theta|0°)+W(\rho,\theta|90°)=T(\rho,\theta)+T(\rho,\theta+90°)+2\cdot W_s(\rho,\theta) \quad (3)$$

$$W(\rho,\theta|0°)+W(\rho,\theta|180°)=T(\rho,\theta)+T(\rho,\theta+180°)+2\cdot W_s(\rho,\theta) \quad (4)$$

For the 36 Zernike terms of W_s (ρ, θ), which can be written as

$$W_s(\rho,\theta)=\sum_{n=0}^{10}\sum_{m=0}^{5}R_n^m(\rho)[a_s^{n,m}\cos m(\theta)+a_s^{n,-m}\sin m(\theta)] \quad (5)$$

we can get the non-rotationally symmetric Zernike coefficients $a_s^{n,4}$ (m=4) by Eq. (2), and similarly get the coefficients $a_s^{n,2}$ (m=2) by Eq. (3), and then get the coefficients $a_s^{n,1}$, $a_s^{n,3}$ and $a_s^{n,5}$ (m=1, 3, 5) by Eq. (4).

However, we cannot precisely ensure the constant system error when this algorithm is applied on grating lateral shearing interferometer. For the schematic of our shearing setup, which is shown in Fig. 1, the beam contains the system wavefront aberration pass through the grating, and we get the shearing interferogram by the ±1 order diffraction lights which are acquired by spatial filter. Due to the working conditions of the shearing interferometer, we always need the large rotating platform to test the system wavefront aberrations of the lens at different angular positions, then it may bring about a large decentration, and may change the whole optical path because of grating shearing. Then the constant system error from the interferometer may also be varied at different rotation angle positions. We can find the size of the decentration by digital image processing (as shown in Fig. 2), but this decentration cannot be simply removed by digital image processing. In addition, and we cannot get the size of variety of system wavefront aberrations by decentration. In this paper, we proposed a three-step average algorithm and a weighted-three-step average algorithm with φ=45° as base point based on single-rotation algorithm [8] to calculate the system error more accurately.

A. Three-step average algorithm with φ=45° as base point

For the combination of 0°-45°, it can be written as:

$$W(\rho,\theta|45°)-W(\rho,\theta|0°)=T_1(\rho,\theta+45°)-T(\rho,\theta) \quad (6)$$

Then the Zernike coefficients of Eq. (6) is:

$$\begin{aligned}&a_{45}(n,\pm m)-a_0(n,\pm m)\\&=a_n^m\cos[m(\theta+45°)]+a_n^{-m}\sin[m(\theta+45°)]\\&-a_n^m\cos[\mathrm{m}(\theta+45°\text{-}45°)]-a_n^{-m}\sin[\mathrm{m}(\theta+45°\text{-}45°)]\\&=A(m,\varphi_1)a_{45}^{T1}(n,\pm m)\end{aligned} \quad (7)$$

Similarly, for the combinations of 45°-90° and 45°-180°, we can get

$$W(\rho,\theta|45°)-W(\rho,\theta|90°)=T_2(\rho,\theta+45°)-T(\rho,\theta+90°) \quad (8)$$

$$W(\rho,\theta|45°)-W(\rho,\theta|180°)=T_3(\rho,\theta+45°)-T(\rho,\theta+180°) \quad (9)$$

Then the Zernike coefficients of Eq. (8) and Eq. (9) are:

$$a_{45}(n,\pm m)-a_{90}(n,\pm m)=A(m,\varphi_2)a_{45}^{T2}(n,\pm m) \quad (10)$$

$$a_{45}(n,\pm m)-a_{180}(n,\pm m)=A(m,\varphi_3)a_{45}^{T3}(n,\pm m) \quad (11)$$

where φ_1=45°, φ_2=45°, φ_3=135°,

$$A(m,\varphi_1)=\begin{bmatrix}\cos m\varphi_1 & \sin m\varphi_1\\ -\sin m\varphi_1 & \cos m\varphi_1-1\end{bmatrix},$$

$$A(m,\varphi_2)=\begin{bmatrix}\cos m\varphi_2 & \sin m\varphi_2\\ -\sin m\varphi_2 & \cos m\varphi_2-1\end{bmatrix},$$

$$A(m,\varphi_3)=\begin{bmatrix}\cos m\varphi_3 & \sin m\varphi_3\\ -\sin m\varphi_3 & \cos m\varphi_3-1\end{bmatrix},$$

and $a_\varphi(n,\pm m)=[a_\varphi(n,m);a_\varphi(n,-m)]$ (φ=0°, 45°, 90°, and 180°), $a_{45}^{T1}(n,\pm m)$, $a_{45}^{T2}(n,\pm m)$, $a_{45}^{T3}(n,\pm m)$ are couples of the Zernike coefficients of W (ρ, θ| φ), T_1 (ρ, θ+45°), T_3 (ρ, θ+45°), and T_3 (ρ, θ+45°).

Due to the real system wavefront aberrations of lens are varied by decentration, there are

$$T_1(\rho,\theta+45°)=T(\rho,\theta+45°)+\Delta W_s'(\rho,\theta), \quad (12)$$

$$T_2(\rho,\theta+45°)=T(\rho,\theta+45°)+\Delta W_s''(\rho,\theta), \quad (13)$$

$$T_3(\rho,\theta+45°)=T(\rho,\theta+45°)+\Delta W_s'''(\rho,\theta)\,. \quad (14)$$

and $\Delta W_s'(\rho,\theta)$, $\Delta W_s''(\rho,\theta)$, $\Delta W_s'''(\rho,\theta)$ are the difference of variable system wavefront aberrations at each angular position.

By Eq. (6)-Eq. (14), we can respectively get three groups of the wavefront aberrations T_1 (ρ, θ+45°), T_3 (ρ, θ+45°), and T_3 (ρ, θ+45°) from the lens under test rotated φ=45°. Then we can get these three groups of system errors by Eq. (15)-Eq. (17)

$$W_{s1}(\rho,\theta)=W(\rho,\theta|45°)-T_1(\rho,\theta+45°) \quad (15)$$

$$W_{s2}(\rho,\theta)=W(\rho,\theta|45°)-T_2(\rho,\theta+45°) \quad (16)$$

$$W_{s3}(\rho,\theta)=W(\rho,\theta|45°)-T_3(\rho,\theta+45°) \quad (17)$$

After that, we process these three groups of system errors by averaging as the final system errors, and the result is

$$W_s(\rho,\theta)=\frac{W_{s1}(\rho,\theta)+W_{s2}(\rho,\theta)+W_{s3}(\rho,\theta)}{3} \quad (18)$$

B. Weighted-three-step average algorithm with φ=45° as base point

In the three-step average algorithm, the measurement positions of wavefront aberrations are asymmetric distribution (0°, 45°, 90°, and 180°). And for the wavefront aberrations acquired from these three combinations (45°-0°, 45°-90°, and 45°-180°), there are positive correlation relationship between the size of variable wavefront aberrations and the rotation angles.

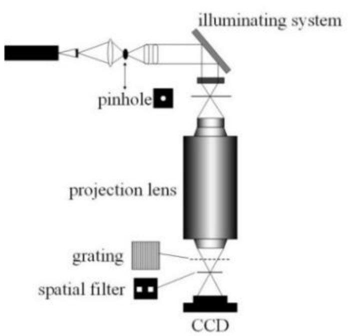

Fig. 1. Schematic of grating lateral shearing interferometer

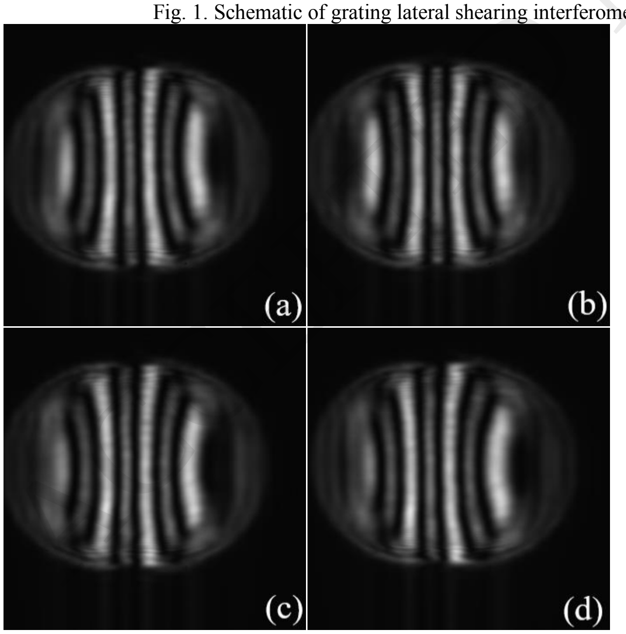

Fig. 2 The interferograms acquired in the experiment when the lens under test are rotated by: (a) 0° (452,489); (b) 45° (443,481); (c) 90° (443,472); (d) 180° (463,460).

Considering this, we proposed a novel weighted algorithm to eliminate the influence of non-uniform measurement, and it means that the measurement results should be weighted by the decentration on these angular combinations.

According to Eq. (12)-Eq. (17), the weighted scheme can be written as:

$$\begin{aligned}
W_s(\rho,\theta) &= \frac{a\cdot W_{S1}(\rho,\theta)+b\cdot W_{S2}(\rho,\theta)+c\cdot W_{S3}(\rho,\theta)}{a+b+c} \\
&= \frac{a\cdot[W(\rho,\theta|45°)-T_1(\rho,\theta+45°)]+b\cdot[W(\rho,\theta|45°)-T_2(\rho,\theta+45°)]+c\cdot[W(\rho,\theta|45°)-T_3(\rho,\theta+45°)]}{a+b+c} \\
&= W(\rho,\theta|45°)-T_1(\rho,\theta+45°)-\frac{a\cdot\Delta W_s{}'(\rho,\theta)+b\cdot\Delta W_s{}''(\rho,\theta)+c\cdot\Delta W_s{}'''(\rho,\theta)}{a+b+c} \\
&= W_{s_real}(\rho,\theta)-\Delta W_s(\rho,\theta)
\end{aligned} \tag{19}$$

where *a, b, and c* represent the weighted coefficient of this method. And we can change the coefficients by the positive correlation relationship between variable wavefront aberrations and the rotation angles to get the $\Delta W_s(\rho,\theta)$ to a minimum. It is

$$\{a,b,c\} = \underset{a,b,c}{\arg\min}\sum_{\rho}\sum_{\theta}\frac{a\cdot\Delta W_s{}'(\rho,\theta)+b\cdot\Delta W_s{}''(\rho,\theta)+c\cdot\Delta W_s{}'''(\rho,\theta)}{a+b+c} \tag{20}$$

Then the constant system errors will be confirmed by this weighted algorithm.

3. EXPERIMENTS

To check the accuracy of three-step average algorithm and weighted-three-step average algorithm, our experiments is implemented on the grating lateral shearing interferometer we researched and developed. The wavelength of optical source is 632.8 nm (λ=632.8 nm). We reconstruct the measured wavefront by the 9-step-phase-shift algorithm [13] and the least-squares technique to process nine couple of lateral shearing interferograms (shown in Fig. 3) in two orthogonal directions. The RMS of the repeatability of experimental data can reach about 0.22mλ.

According to these three methods in this paper, we respectively acquire the lateral shearing interferograms of the lens under test at original position and the positions by rotating 45°, 90°, 180°, and φ_i (a random angle about 300°).

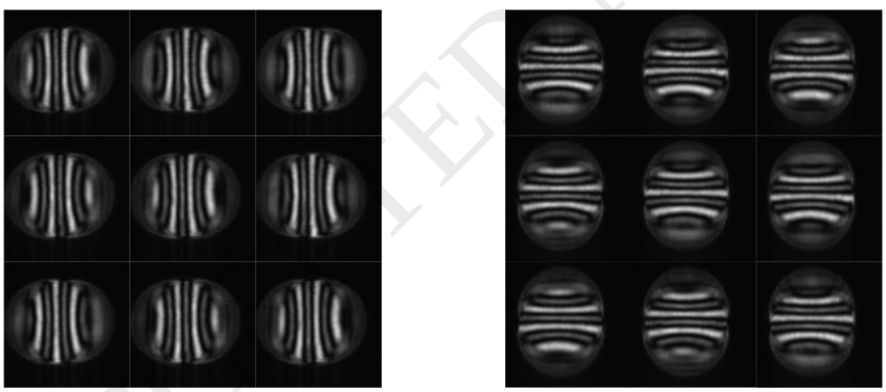

Fig. 3 The lateral shearing interferograms in orthogonal directions

φ（°）	The total wavefront aberrations	Three-step combination algorithm	Three-step average algorithm	Weighted-three-step average algorithm
0	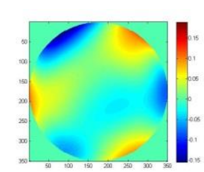	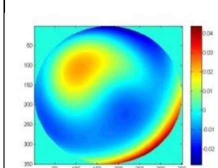	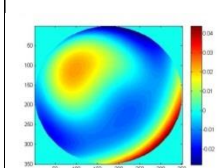	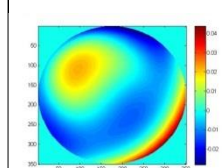

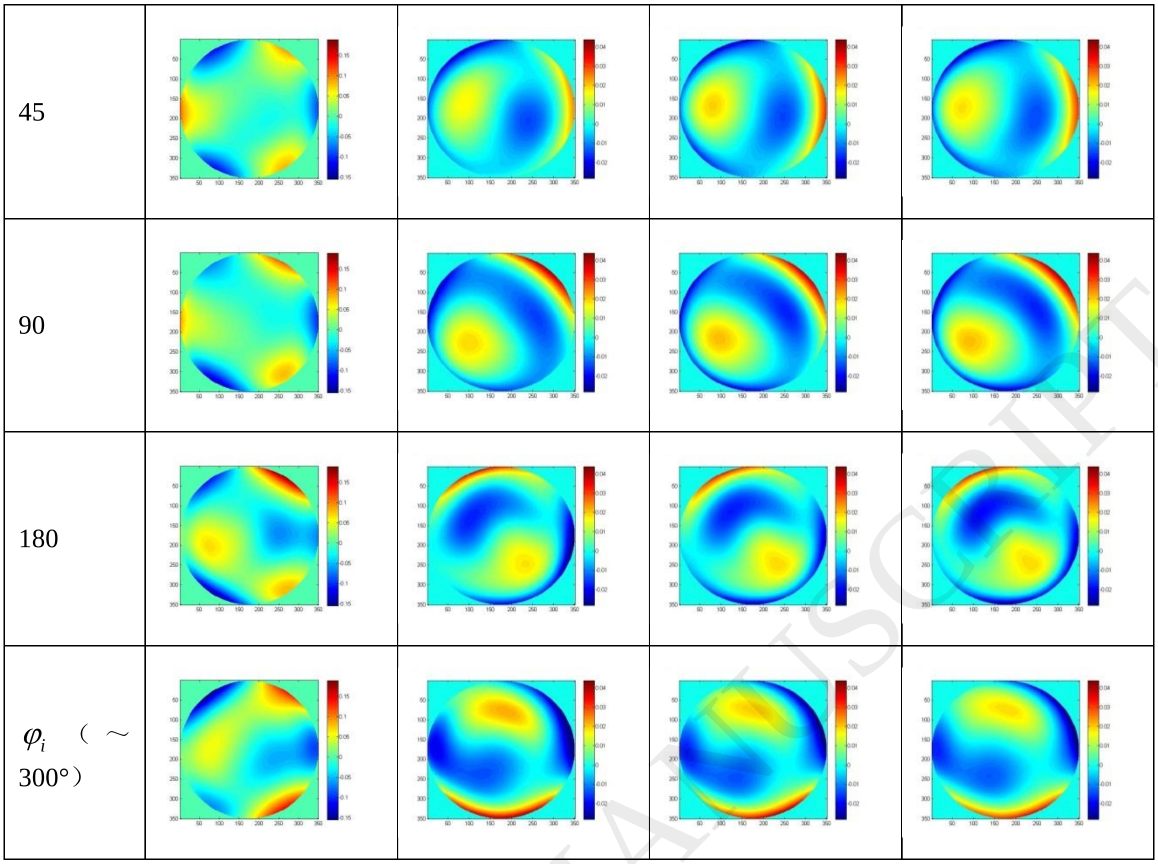

Fig. 4 The results before system errors elimination and after system errors elimination (The total wavefront aberrations and the results under these three algorithms)

After wavefront reconstruction, we get five wavefront aberrations $W(\rho, \theta| \varphi)$ with system errors. Then we separately utilize the three-step combination algorithm [4], three-step average algorithm, and weighted-three-step average algorithm to separate the rotationally asymmetric system errors, and validate the accuracy of these three algorithms by a random angle about 300°. The total wavefront aberrations and the results under these three algorithms are shown in Fig. 4, and the RMS values of the wavefront aberrations of the lens under test are shown in Tab. 1.

As we can see the contrast from Fig. 4 and Tab. 1, the RMS of the measurement precision of the three-step average algorithm with φ=45° as base point we developed in this paper can reach about 0.71nm, and it will reach about 0.54nm by weighted-three-step average algorithm.

Tab. 1 The RMS values of the wavefront aberrations from the lens under test

φ（°）	**Before system errors elimination** （λ）	**After system errors elimination** （λ）		
		Three-step combination algorithm	Three-step average algorithm	Weighted-three-step average algorithm
0	0.041775	0.011993	0.013276	0.012371
45	0.036954	0.008873	0.010158	0.010041
90	0.036907	0.011463	0.011656	0.012170
180	0.046559	0.010670	0.010506	0.010908
φ_i **（～300°）**	0.047385	0.013221	0.012112	0.011447
Precision measurement（RMS）	0.004500	0.001440	0.001120	0.000850

4. CONCLUSION

We have presented two simple and effective methods for rotationally asymmetric system errors correction. These different methods are based on the non-uniform sampling of three-step combination algorithm [4]. In this paper, we have revealed the different results from these three methods. By contrast, three-step average algorithm with φ=45° as base point is a high-efficiency and high-accuracy method to eliminate the system errors, and weighted-three-step average algorithm is a new method can solve the problem of non-uniform sampling. Furthermore, these two methods we proposed can be applied to most of absolute measurement technology.

Funding

Ministry of Science and Technology of the People's Republic of China (MOST);
The 02 National Science and Technology Major Project (2009ZX02202005).

REFERENCES

1. J. Bueno, E. Acosta, C. Schwarz, "Wavefront measurements of phase plates combining a point-diffraction interferometer and a Hartmann-Shack sensor," Appl. Opt. 49, 450-456 (2010).
2. C. Ouchi, S. Katoa, M. Hasegawa, "EUV wavefront metrology at EUVA," SPIE. 6152:61522 (2006).
3. H. Schreiber and J. Schwider, "Lateral shearing interferometer based on two Ronchi gratings in series," Appl. Opt. 36, 5321-5324 (1997).
4. S. Mack, T. Rich, J. Webb, P. Dewa, H. Schreiber, "Error separation technique for microlithographic lens testing with null configurations," Proc. SPIE 4346, 1328-1339 (2001).
5. T. Hasegawa, C. Ouchi, M. Hasegawa, S. Kato and A. Suzuki, "EUV Wavefront Metrology System in EUVA", SPIE 5374, 797-807 (2004).
6. D. Su, E. Miao, Y. Sui, and H. Yang, "Absolute surface figure testing by shift-rotation method using Zernike polynomials," Opt Letters 37, 3198-3200 (2012).
7. D. Malacara, Optical Shop Testing (Wiley, 1992).
8. R. E. Parks, "Removal of test optics errors," Proc. SPIE 153, 56–63 (1978).
9. K. Creath and J. C. Wyant, "Testing spherical surfaces: a fast, quasiabsolute technique," Appl. Opt. 31, 4350–4354 (1992).
10. C. J. Evans, R. N. Kestner, "Test optics error removal," Appl. Opt. 35, 1015-1021 (1996).
11. W. Wang, M. Zhang, S. Yan, Z. Fan, and J. Tan, "Absolute spherical surface metrology by differencing rotation maps," Appl. Opt. 54, 6186-6189 (2015).
12. W. Song, F. Wu, and X. Hou, "Method to test rotationally asymmetric surface deviation with high accuracy," Appl. Opt. 51, 5567–5572 (2012)
13. Y. Zhu, Y. Su, Y. Chen, "Lateral shearing interferometer for EUVL: theoretical analysis and experiment," SPIE 5374, 824-832 (2004).